

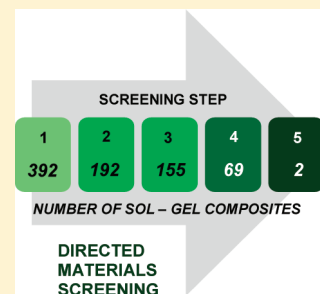
# Materials Screening for Sol–Gel-Derived High-Density Multi-Kinase Microarrays

Xin Ge,<sup>†</sup> Julie M. Lebert, Maria Rowena N. Monton, Laura L. Lautens, and John D. Brennan\*

Department of Chemistry and Chemical Biology, McMaster University 1280 Main St. W, Hamilton, Ontario L8S 4M1, Canada

**S** Supporting Information

**ABSTRACT:** Protein microarrays based on pin-printing of sol–gel-entrapped biomolecules have emerged as a potential tool to accelerate drug screening and discovery. However, while materials have recently been identified that are suitable for printing of high-density sol–gel-based microarrays, the ability to print arrays of delicate proteins such as kinases, and to assay their activity and inhibition on-array, has yet to be demonstrated. In this study, we have performed a criteria-based directed screen of sol–gel-based materials to identify compositions that are suitable for the fabrication of high-density, multikinase microarrays. Printable formulations were assessed for their compatibility with a fluorescent, phosphospecific dye used as an end-point indicator for on-array kinase assays, including an assessment of the effects of spot size (100  $\mu\text{m}$  vs 400  $\mu\text{m}$ ) and slide surface chemistry on signal reproducibility. The combinations of materials, surfaces, and spot sizes that were found to be compatible with reproducible signal generation were evaluated for their ability to retain the activity of a range of kinases, which were co-entrapped with their respective substrates into the optimal sol–gel materials to produce microarrays. Ultimately, two material/surface combinations, from potentially thousands, were identified, one of which was used to produce a robust, highly active kinase microarray that could be used for qualitative screening as well as quantitative inhibition assays.



**KEYWORDS:** materials screening, sol–gel, pin-printing, microarray, kinase, high-throughput screening

## INTRODUCTION

Protein kinases are a family of enzymes that catalyze the transfer of the  $\gamma$ -phosphate group from ATP to serine, threonine, or tyrosine residues in target protein or peptide substrates.<sup>1</sup> These phosphorylation events are involved in countless signaling pathways and cellular processes.<sup>2</sup> Improper regulation of kinase activity has been implicated in many diseases, such as cancer,<sup>3</sup> inflammation,<sup>4</sup> and diabetes.<sup>5</sup> Consequently, it is widely acknowledged that modulation of kinase activity offers potential therapeutic value for the treatment of these diseases,<sup>6</sup> and kinases have emerged as one of the most important target classes for drug discovery.

For assessing kinase activity and inhibition, the transition from standard solution-phase assays to immobilized formats has markedly increased assay throughput and decreased reagent consumption. Kinase microarrays<sup>8–14</sup> can screen hundreds of samples at nanoliter volumes in a highly parallel manner, allowing for relatively fast, easy, and inexpensive determination of kinase action on numerous substrates at once.<sup>15</sup>

An emerging method of preparing functional protein microarrays involves the pin-printing of protein-doped silica sols onto functionalized surfaces, which subsequently gel and entrap the protein in a three-dimensional silica network.<sup>15–19</sup> Because the protein is not artificially tethered to the surface, sol–gel entrapment eliminates the need for protein derivatization and minimizes the potential for loss of activity due to improper orientation.<sup>15</sup> The method is amenable to a wide variety of proteins,<sup>20–22</sup> affords high protein loading,<sup>23</sup> and enables co-entrapment of multiple proteins in the same sol–gel matrix,

enabling coupled enzyme reactions and reagentless biosensing.<sup>24–26</sup> Furthermore, it is possible to control the properties of the matrix through judicious choice of silica precursor and additives in order to optimize protein activity.<sup>27</sup>

The development of sol–gel-based microarray technology into a robust, highly scalable platform for low-volume, multi-point, high-throughput screening depends on the selection of suitable matrix materials. In lieu of a costly, time-consuming comprehensive screen, a small, directed screen can often be used to identify optimal materials for producing high-density microarrays, as we have demonstrated in a recent report.<sup>27</sup> This focused strategy restricted the selection of materials and processing conditions for evaluation only to those that were previously shown to be amenable to array fabrication and retention of enzyme activity, and screening was performed based on systematic hierarchical fulfillment of selected criteria. In this way, from a total of  $\sim 20\,000$  potential formulations, a small subset of materials/surface combinations that could produce robust, highly active acetylcholinesterase (AChE) microarrays was rapidly identified.

In this work, we extend the sol–gel materials screening approach to identify materials that are suitable for the preparation of high-density, multikinase microarrays. We previously reported on an array-based assay for kinase activity using the

**Received:** April 30, 2011

**Revised:** July 17, 2011

**Published:** July 28, 2011

$\alpha$ -catalytic subunit of cAMP-dependent protein kinase A and its peptide substrate kemptide coimmobilized within a sol–gel material as models, and the phosphospecific dye Pro-Q Diamond as an end-point indicator for phosphorylation.<sup>15</sup> While the utility of this technique for monitoring kinase activity and inhibition was clearly demonstrated, its potential as a high-throughput screening platform was not easily realized, because it was not possible to produce either higher density or multikinase arrays using the original sodium silicate starting material, owing to rapid gelation and inadequate activity for other kinases.

Herein, we report on a directed materials screening method for identifying optimal sol–gel composites for the fabrication of high-density, multikinase microarrays, with the range of targets expanded to include both soluble and membrane-associated kinases. A two-stage, multistep approach, which involves primary screening for material properties (gelation time and printability) and secondary screening for assay suitability (compatibility with detection method and retention of enzyme activity), demonstrates the effectiveness of a criteria-directed screening method for rapid and efficient optimization of materials for specific applications.

## EXPERIMENTAL SECTION

**Materials.** Sodium silicate (SS, 27 wt % SiO<sub>2</sub>, 10 wt % NaOH) was purchased from Fisher (Ottawa, ON, Canada). Diglycylsilane (DGS) was prepared as previously described from tetramethyloctosilicate (TMOS) (Sigma–Aldrich, Oakville, ON, Canada) and anhydrous glycerol (Sigma–Aldrich).<sup>28</sup> Bis[(3-methyldimethoxysilyl)propyl]polypropylene oxide (MDSPPO), *N*-(3-triethoxysilylpropyl) gluconamide (GLS), aminopropyltriethoxysilane (APTES), bis-(triethoxysilyl) ethane (Bis-TEOS), phenyldimethylsilane (PhDMS), and carboxyethyl silanetriol (Si-COOH) were purchased from Gelest (Morrisville, PA). Sorbitol, trehalose, *N*-acetyl-lysine, Triton X-100, magnesium chloride, manganese chloride, ATP,  $\beta$ -nicotinamide adenine dinucleotide, reduced (NADH), phospho(enol)pyruvate (PEP), poly(vinyl alcohol) (PVA, MW = 9000), polyethylene imine (PEI, MW = 1300), polyethylene glycol (PEG, MW = 600),  $\beta$ -casein, bovine serum albumin (BSA), pyruvate kinase from rabbit muscle (PK), D-lactic dehydrogenase from *Lactobacillus leichmanii* (LDH), poly(Glu<sub>4</sub>Tyr) (p(E<sub>4</sub>Y)), and Dowex 50WX8-100 ion-exchange resin were obtained from Sigma–Aldrich. The kinases p38 $\alpha$ /SAPK2 $\alpha$  (p38 $\alpha$ ), mitogen-activated protein kinase 2/Erk2 (MAPK2), epidermal growth factor receptor (EGFR), and glycogen synthase kinase 3 $\beta$  (GSK-3 $\beta$ ), the substrates myelin basic protein (MBP), the GSK-3 $\beta$  substrate peptide GSM, and the inhibitor staurosporine were donated by Millipore (Billerica, MA). The kinases and substrates were used at the following kinase/substrate pairings: p38 $\alpha$ /MBP, MAPK2/MBP, EGFR/p(E<sub>4</sub>Y), GSK-3 $\beta$ /GSM. Pro-Q Diamond staining and destaining solutions were purchased from Invitrogen (Burlington, ON, Canada). The derivatized microscope slides and stealth pins for contact pin-printing were purchased from ArrayIt (Sunnyvale, CA). Poly(methyl methacrylate) (PMMA) slides were obtained from Exakt Technologies (Oklahoma City, OK). Water was purified using a Milli-Q Synthesis A10 water purification system (water from this system was identified as ddH<sub>2</sub>O). All other chemicals and solvents were of analytical grade and were used without further purification.

**Materials Screening.** Details of the procedures used to screen materials are provided in the Supporting Information. Briefly, composites resulting from the combination of two silica precursors (SS and DGS) at two concentrations (1.4 and 2.8 for SS, 2.5 and 5.0 for DGS, in terms of wt % SiO<sub>2</sub>), three polymers (PVA, PEG, PEI) at two concentrations (0.5% and 1.0% w/v for PVA and PEI, 3.8% and 7.5% w/v for

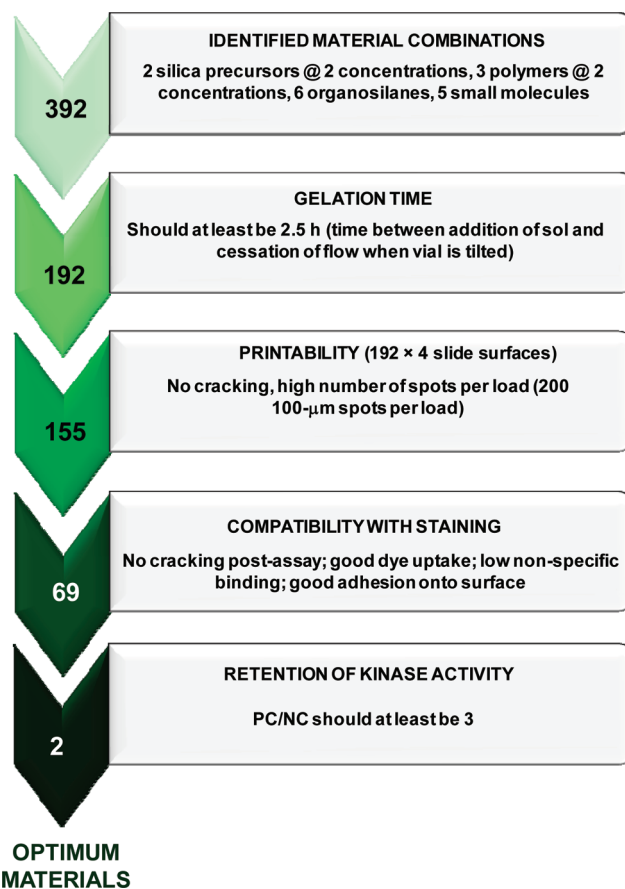


**Figure 1.** Directed materials screening approach for identification of optimal materials for fabricating sol–gel-derived kinase microarrays.

PEG), six organosilanes (MDSPPO, Bis-TEOS, PhDMS, GLS, APTES, Si-COOH), and five small-molecule additives (glycerol, sorbitol, trehalose, *N*-acetyl L-lysine, and Triton X-100) were produced at a single buffer composition (25 mM HEPES, pH 8.0), which was optimized to produce long gelation times and entrap proteins at neutral pH. Suitable sols, which exhibited gelation times longer than 2.5 h, were printed onto four different functionalized surfaces (aldehyde-, amine-, and epoxy-modified glass slides and PMMA) and assessed for printability. Two sets of microarrays were prepared from each printable formulation—one with the model phosphoprotein,  $\beta$ -casein, and the other without—and both were assessed for compatibility with Pro-Q Diamond<sup>29</sup> by evaluating reproducibility of spot diameters, cracking of the spots, adherence of spots to the surface, and signal-to-background (S/B) ratios. Compositions that passed the minimum material property requirements were then assayed for kinase activity against the four kinase targets. From those that were able to retain high kinase activity, one material was selected for microarray fabrication. The attrition of materials upon moving through the different screening steps is shown in Figure 1.

**Functional Kinase Microarrays.** Spotting solutions consisting of an optimal sol–gel material (1.4SS/1.0PVA) and containing the kinases and their respective substrates were printed (see the Supporting Information for details on nomenclature and printing of microarrays) onto an amine-derivatized slide as arrays of 100- $\mu$ m spots using an SMP3 pin (250 nL uptake, 0.7 nL delivery; 350 spots/loading). For a typical reaction volume of 40  $\mu$ L, 3–7 U of kinases were added, and the final concentrations of the substrates were 27  $\mu$ M MBP, 5 mg/mL p(E<sub>4</sub>Y), and 37.5  $\mu$ M GSM. For optimum results, the kinase was added to the sol immediately before printing. After printing, the spots were allowed to age for 30 min inside a high-humidity chamber (~80% relative

humidity) prior to being used in activity or inhibition assays. For activity assays, the spots were overprinted with 100  $\mu$ M ATP and 10 mM MgCl<sub>2</sub> in 50 mM Tris-HCl, pH 7.5, using a larger SMP7 pin (250 nL uptake, 2.3 nL delivery; 100 spots/loading) to ensure complete coverage. For inhibition assays and IC<sub>50</sub> measurements, the overspotting solution contained, in addition to ATP and the metal ion cofactor, varying concentrations of the general kinase inhibitor staurosporine straddling its known IC<sub>50</sub> value. The reactions were allowed to proceed for 2 h inside a high-humidity chamber, after which the arrays were stained, destained, imaged, and analyzed as described in the Supporting Information.

## RESULTS AND DISCUSSION

**Materials Screening.** One of the most significant challenges in producing pin-printed microarrays is poor spot size reproducibility, particularly of 100- $\mu$ m array elements, which can be attributed to the inability to control the deposition volume from stealth pins. Regardless of the sol–gel material or the slide surface chemistry, the first  $\sim$ 50 spots tend to be larger than the rest (see Figure S1A in the Supporting Information), likely because of a large pressure head at the beginning of a printing cycle or the presence of residual spotting solution around the exterior of the pin, which must be exhausted first before the deposited volumes become consistent. This problem could be overcome by blotting the first 50–70 spots onto a separate surface prior to printing arrays. However, such a method is wasteful, in terms of both time and reagents. Interestingly, the use of a larger pin to produce 400- or 600- $\mu$ m spots did not have issues with spot size reproducibility (see Figure S1B in the Supporting Information), although using such pins came at the expense of reduced array density, as fewer spots could be printed within a given area. Figure S2 in the Supporting Information shows typical data obtained from an alternating array of positive controls (PC,  $\beta$ -casein) and negative controls (NC, BSA) for 1.4SS/1.0PVA microarrays printed on an amine surface, and reveals several key findings:

- (1) The fluorescence intensity of PCs is typically 2–3 fold higher than that for NCs;
- (2) The intensity values over the first 50 spots are highly irreproducible; and
- (3) The intensity over the latter 150 spots is sufficiently reproducible to allow for screening applications ( $Z'$  values typically in the range of 0.6–0.7 for most arrays, using spots 51–200).

Many SS-based materials with high silica concentrations (2.8SS) exhibited poor spot deposition and uniformity, or even pin clogging, because they were more likely to undergo more-rapid viscosity changes. As a result, inconsistencies in deposited volumes were observed during the printing process. In contrast, all DGS-based compositions showed excellent printability. The addition of the surfactant Triton X-100 resulted in spots that were significantly larger than those formed using other formulations, regardless of the surface on which they were printed, while the presence of the organosilane GLS, which imparts some degree of hydrophobicity to the spotting solution, resulted in smaller spots. All other organosilane additives produced materials that were not printable, because of insufficient gelation times.

For sol–gel-derived protein microarrays, unlike in other immobilization techniques, the surface chemistry of the underlying slide does not profoundly affect the activity of the entrapped biomolecule, as the protein does not directly interact

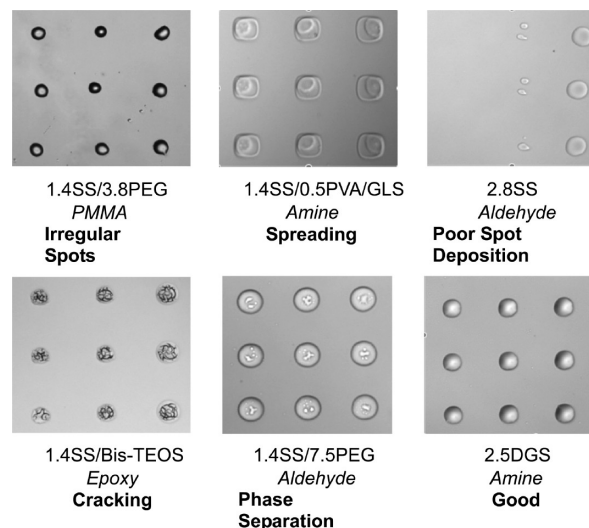


**Figure 2.** Optical images showing various failure modes of materials at the printability step of the screening. An image of a “good” material (second row, third column) is also shown for comparison.

with the substrate. However, surface chemistry does influence printing of the spots. Printing was usually best on amine-functionalized surfaces, slightly worse on epoxy surfaces, worse still on aldehyde surfaces, and very poor on PMMA (note that studies on PMMA surfaces were terminated at this point). Amine and epoxy, being more polar, were better-suited to aqueous sols. Spots that were printed onto aldehyde were smaller than their counterparts printed on other surfaces, which also is likely a reflection of the higher hydrophobicity of this surface, which limited spreading of sols.

Using the criterion that a sol/surface combination must allow printing of at least 200 spots 100  $\mu$ m in diameter without cracking in a single pin loading in order to be considered “printable”, 155 materials/surface combinations were considered to be satisfactory. Figure 2 shows a selection of optical micrographs of arrays formed with different sol–gel materials on different slide surfaces, and provides an indication of the various failure modes that were observed.

**Staining Compatibility Studies.** From the printable combinations, a subset of 26 were previously identified as being amenable to fabricating active AChE microarrays, with the end-point of the assay indicated by a fluorogenic BODIPY dye.<sup>27</sup> While this list could serve as a useful guide as to the composition of materials suitable for both pin-printing and successful enzyme entrapment, it could not be readily extended to kinases, because of differences between enzymes, as well as specific assay requirements. A key dissimilarity exists between the AChE assay and the kinase assay described in the present work, how the indicator reagent is delivered to the reaction site, which can impact the selection of suitable matrix materials and slide surface chemistry. In the AChE assay, nanoliter aliquots of the BODIPY indicator dye were directly deposited over individual array elements by overprinting. On the other hand, in the kinase assay, the entire slide is immersed sequentially in the staining and destaining solutions, and then water. The prolonged exposure of spots to copious amounts of liquids puts greater emphasis on finding materials with an appropriate pore size and distribution, and amplifies the effect of surface chemistry, which can result in either high background signals resulting from nonspecific binding of the



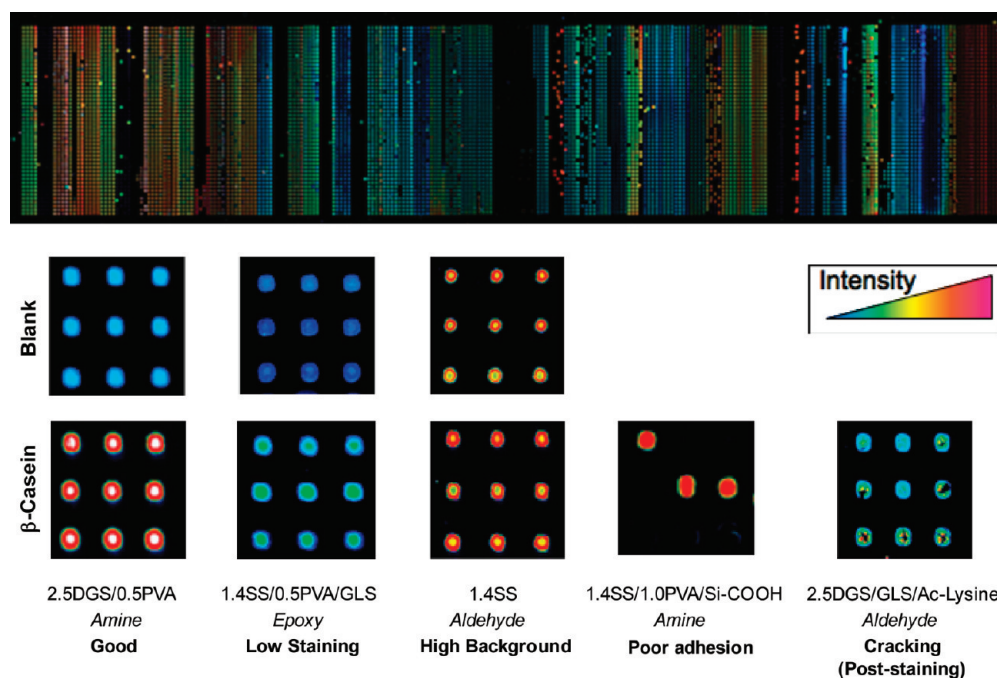


**Figure 3.** A 12 000-spot microarray (60 samples  $\times$  200 spots/sample) printed onto an amine-derivatized slide, with insets illustrating different failure modes observed at the stain compatibility step of the screening. Images from a “good” material (first column) are also shown for comparison.

dye, or a loss of spots, because of cracking related to hydration stress<sup>30</sup> brought about by inhomogeneous capillary pressure.<sup>31</sup> The extensive staining, destaining and washing steps can also increase the possibility of the protein leaching from the gel. Thus, the material should have a narrow pore size distribution to minimize capillary stress, and the pores should be large, yet small enough to work as nanocages, preventing the protein from leaching out of the gel.

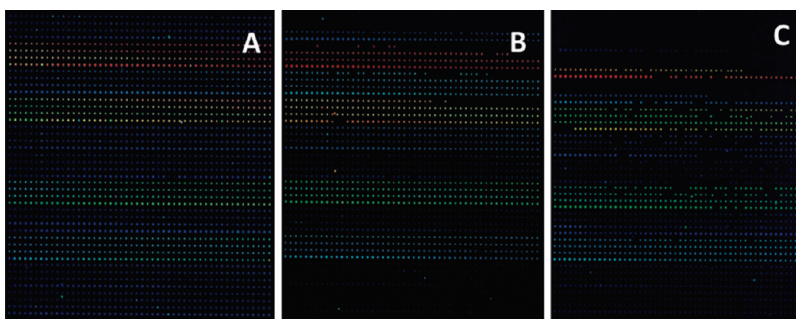
As the assay reporter for phosphorylation, we used the commercial phosphostaining dye Pro-Q Diamond, which is an iron(II) chelating complex linked to a rhodamine fluorophore that specifically binds to O-linked phosphorylated amino acids (serine, tyrosine, threonine), forming a bridge between the phosphorylated amino acid and the Rhodamine dye.<sup>27,29</sup> As noted above, the staining process involves immersing the microarrays in the dye, followed by washing with a moderately acidic destaining solution to remove unbound and nonspecifically bound dye. Successful use of this stain requires that the dye can access and bind to the phosphorylated sites in the array elements, while not binding strongly to the matrix. The optimal material should allow for large signal, because of binding of the dye to phosphorylated species, and low background, arising from nonspecific binding of the dye. Evaluation of the stained/destained arrays, formed using the 155 material/surface combinations, was performed by comparing the S/B ratio between two sets of microarrays prepared from each printable formulation: one with the model protein,  $\beta$ -casein, which contains five phosphoserine residues (S), and the other without (B). The higher the resulting S/B ratios are, the better the materials. In addition, the spots were assessed for the presence of cracking and adhesion to the surface post-assay.

Figure 3 shows a typical high-density, 12 000-spot microarray-based materials screening result, in this case, for arrays of 60 materials (of the 155) printed on an amine-functionalized slide, with illustrative examples of various failure modes shown in the

insets. At this point, a number of material/surface combinations were eliminated, because of poor staining, high background levels, cracking, and/or poor adhesion of microarray elements to the surface. From these data, it was possible to make several observations. PEG-modified materials were observed to have poor S/B ratios, suggesting that this polymer blocked access to the phosphorylated substrate or allowed extensive leaching of the substrate. In contrast, the addition of PVA, GLS, glycerol, or sorbitol resulted in better binding of the dye by  $\beta$ -casein, while not significantly affecting the background. Figure S3 in the Supporting Information shows both SEM and AFM images of typical PVA- and PEG-modified materials, and confirms that the pore size for the PVA-doped material was smaller than that of the PEG-doped material. Based on this observation, it is likely that the more macroporous PEG-doped materials lead to leaching of the phosphorylated protein, thereby reducing the signal intensity.

A major issue with DGS-based materials was the cracking of materials with high silica content (5.0DGS); this was also a problem for those materials that contained PEG and GLS. However, the presence of PVA clearly appeared to protect against cracking. Inspection of Figure S3 in the Supporting Information demonstrates that the PVA materials are very homogeneous, while the PEG-modified materials are more heterogeneous in terms of pore size and, thus, may be more prone to capillary stresses. Poor adhesion was not a very common problem (as this parameter had already been part of the primary screen), except in compositions containing Si-COOH.

From the above screen, a total of 69 material/surface combinations (29 materials spread across three surfaces) passed this screening step. Using 25  $\mu$ M  $\beta$ -casein (corresponding to  $\sim$ 125  $\mu$ M phosphorylation sites), S/B ratios in the 10–15 range were obtained, without the necessity of blocking unused surfaces prior to staining in order to minimize nonspecific binding. Given that most kinases have  $K_M$  values in the range of 100–200  $\mu$ M



**Figure 4.** Alternating arrays (200 spots/array,  $4 \times 50$  pattern) of the 1.4SS/1.0PVA material containing entrapped  $\beta$ -casein (positive control) or BSA (negative control) printed onto (A) amine-, (B) epoxy-, and (C) aldehyde-modified surfaces after staining with Pro-Q Diamond. The intensity gradient is identical to that shown in Figure 3.

and, for most assays, a turnover of 10%–20% is desirable, these materials should enable S/B ratios of 2–3 for typical on-array assays (although this could be improved by using higher substrate concentrations, at the expense of missing weaker competitive inhibitors). To assess the reproducibility of printing and staining, 1600-spot arrays, consisting of alternating arrays of 200 spots of a positive ( $\beta$ -casein) and negative (BSA) control, were printed for each of the 69 material/surface combinations, followed by staining, destaining, and imaging. Figure 4 shows a representative set of data for the 1.4SS/1.0PVA material printed onto (A) amine-, (B) epoxy-, and (C) aldehyde-derivatized surfaces. The data show that the amine surface was the best for the on-array kinase assay that utilized Pro-Q Diamond as an end-point indicator, with the epoxy surface being almost as good, and the aldehyde being the worst (i.e., amine  $\geq$  epoxy  $\gg$  aldehyde). The frequency of missing spots was lowest on the amine surface, likely because of strong electrostatic interaction between the positively charged amine groups on the surface and the negatively charged silanol sites in the silica matrix, which prevent the spots from being removed easily during the repeated wash cycles. In addition, the background levels with the stain were lowest on amine surfaces, likely because the cationic dye was less prone to adsorb onto a similarly charged surface.

**Kinase Activity in Monoliths.** Previous studies of sol–gel-based kinase microarrays required relatively high loadings of the kinase (PKA) in order to obtain reasonable activity (1  $\mu$ g or 50 U of 50 000 U/mg kinase in the spotting well).<sup>15</sup> Given that many of the kinases studied herein had much lower activity (300–700 U/mg activity for the four kinases), we chose to assay each of the four kinases at a macroscopic scale for each of the 29 materials using 50  $\mu$ L of each sol–gel-derived material in a 96-well plate-based assay format prior to assessing kinase activity on microarrays (microplate format requires 0.1  $\mu$ g of protein per assay, microarray method requires initial mass of  $\sim 10$   $\mu$ g in the spotting well). Four kinases, p38 $\alpha$ , MAPK2, EGFR and GSK-3 $\beta$ , were selected based on their therapeutic relevance: kinases p38 $\alpha$  and MAPK2 are known anticancer targets;<sup>32,33</sup> GSK-3 $\beta$  is an important target for the treatment of diabetes and Alzheimer's Disease;<sup>34</sup> and EGFR is a membrane-associated kinase that is overexpressed in tumor cells, and thus provides a useful demonstration of the extension of the microarray technology to membrane-associated kinases.<sup>35</sup> Thus, all four are excellent candidates for assay development.

Kinase activity was assessed using a coupled NADH assay,<sup>36</sup> because it was not possible to adequately stain and destain the larger monolithic gels, owing to the time required for diffusion of

the dye into and out of the material (several days). Absorbance at 340 nm was monitored over a 1-h period and the ratios between the rates of absorbance decrease between PC (with ATP) and NC (no ATP) samples were determined, with materials showing high ratios considered to be able to retain kinase activity. A summary of results of this screening step is shown in Table S1 in the Supporting Information. Several kinases retained activity in materials containing GLS, a trend previously observed for Src tyrosine kinase.<sup>37</sup> Unfortunately, no material could retain the activity of all four kinases in monolith-based assays, although two materials, 1.4SS/1.0PVA/Glycerol and 2.SDGS, were shown to retain activity for three of the four kinases, with the former showing the highest retention of activity (see Figure S4 in the Supporting Information). Interestingly, the 1.4SS/1.0PVA/Glycerol material was also found to be one of the optimal sol compositions for fabricating active AChE microarrays,<sup>27</sup> suggesting that this material may be amenable to entrapment of a wide variety of proteins.

**Functional Kinase Microarrays.** Preliminary microarray-based assays utilized the two materials that were identified in monolith-based assays, and these were printed onto amine-derivatized slides, because these surfaces had previously been identified as being the most compatible with these materials. In addition to the two materials identified in monolith-based assays, we also assessed several related materials that showed activity for at least two of the kinases, as well as the 1.4SS/1.0PVA material without glycerol, as the material with glycerol added did not form reproducible spots when printing with the SMP3 pin. Of these materials, the 1.4SS/1.0PVA material on amine-derivatized slides was the only one to show activity for all four kinases, with the 2.SDGS material showing activity for only three kinases (not EGFR) and a lower S/B ratio. For this reason, all remaining studies were performed with the 1.4SS/1.0PVA material printed on amine-derivatized slides.

Prior to performing on-array activity assays, we first assessed whether the 1.4SS/1.0PVA material exhibited a quantitative response with Pro-Q Diamond. By plotting fluorescence intensity vs. concentration of  $\beta$ -casein spanning a  $\sim 100$ -fold concentration range (0.25–25  $\mu$ M), the linearity coefficients obtained were  $\sim 0.97$ , attesting to the suitability of the materials for quantitative assessment of phosphorylation in on-array assays, as shown in Figure S5 in the Supporting Information.

The kinases GSK-3 $\beta$ , EGFR, MAPK2, and p38 $\alpha$ , and their respective substrates, were incorporated in 1.4SS/1.0PVA and printed onto an amine-derivatized slide. After gelation and aging, the spots were overprinted with 50 mM Tris-HCl, pH 7.5, or with

solutions containing 100  $\mu\text{M}$  ATP and 10 mM  $\text{MgCl}_2$  in 50 mM Tris-HCl, pH 7.5, with or without the inhibitor staurosporine. A section of the microarray scanned after 2 h of incubation is shown in Figure 5. The fluorescence intensities of spots overprinted with ATP (PC, middle row) were considerably higher than those overprinted with buffer alone (NC, top row). The resulting PC/NC ratios were 4.5 (p38 $\alpha$ ), 3.7 (MAPK), 1.9 (EGFR), and 4.0 (GSK-3 $\beta$ ), with the lower PC/NC for EGFR likely a reflection of lower activity for the membrane-associated kinase relative to the soluble kinases. On the other hand, there was a reduction in intensity for spots that were overprinted with ATP and staurosporine (inhibited reaction, bottom row). These results clearly demonstrate that (i) all four kinases remained active in the sol–gel-derived spots and (ii) the kinases were all sensitive to the presence of the inhibitor staurosporine.

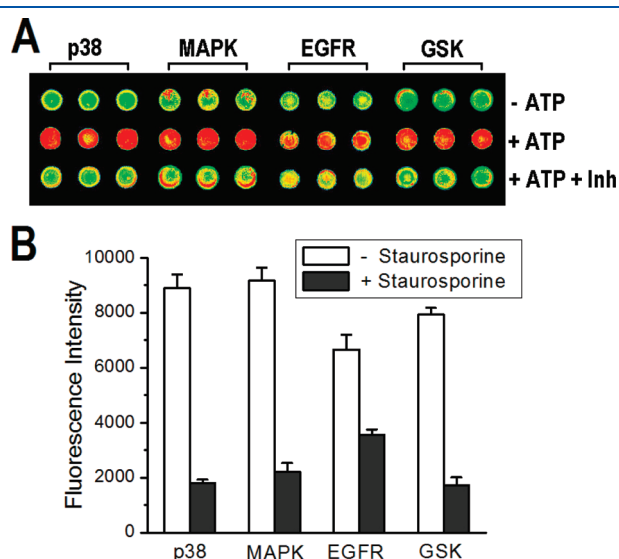


**Figure 5.** On-array assay of four kinases using 1.4SS/1.0PVA for entrapment and printed onto an amine-derivatized slide. Panel A shows an image of a section of microarray in which spots with kinases co-entrapped with their respective substrates were overprinted with buffer (NC, top row), or solutions containing ATP (PC, middle row) or ATP + staurosporine (bottom row). Panel B shows bar graphs comparing signal intensities between inhibited and uninhibited reactions, after the subtraction of background signals. Intensity gradient is identical to that shown in Figure 3.

To evaluate the utility of microarrays for providing quantitative inhibition data, the kinase p38 $\alpha$  was co-entrapped with MBP in 1.4SS/1.0PVA and used as a test system. To generate a concentration-dependent inhibition curve, different rows of spots were incubated with varying concentrations of staurosporine, while keeping the ATP concentration constant. The  $\text{IC}_{50}$  curve resulting from analysis of the microarray is shown in Figure 6. Clearly, the signals relate inversely to the inhibitor concentration, and the  $\text{IC}_{50}$  value was calculated to be  $\sim 1 \mu\text{M}$ .

Overall, the optimal material for kinase microarray fabrication that was identified from the criteria-based multiparameter screen was shown to be printable, compatible with the phosphostaining detection method, able to retain enzyme activity, and could be used qualitatively (to determine kinase activity or inhibition) and quantitatively (to determine potency of an inhibitor). The results in this study underscore three important points, as far as optimal material compositions are concerned:

- (1) As a silica precursor, SS is the most amenable to the production of reproducible microarrays, in agreement with results obtained in previous studies;<sup>23,27</sup>
- (2) The key additive to obtain useful sol–gel-based microarrays is the polymer PVA. This multifunctional hydroxylated additive can improve spot morphology, homogeneity of distribution, and uniformity of signal response, as demonstrated herein and previously in antibody microarrays,<sup>38</sup> and can control porosity and protect against drying-induced denaturation; and
- (3) The most suitable surface for printing sol–gel-derived microarrays is amine.

The identification of these materials should help move sol–gel-derived microarrays forward as a platform for nanovolume, high-throughput assays.

## CONCLUSIONS

The present study provides a further demonstration of the usefulness of a directed screening methodology, in this case to identify sol–gel compositions that can be used for the fabrication of high-density kinase microarrays via the pin-printing method. By using a criteria-directed screen and assessing the variables in a stepwise fashion, the actual number of material combinations that needed to be evaluated could be drastically reduced, along with associated time and cost, while not compromising the likelihood of identifying the optimal materials. Importantly, this study highlights the importance of customizing the selection

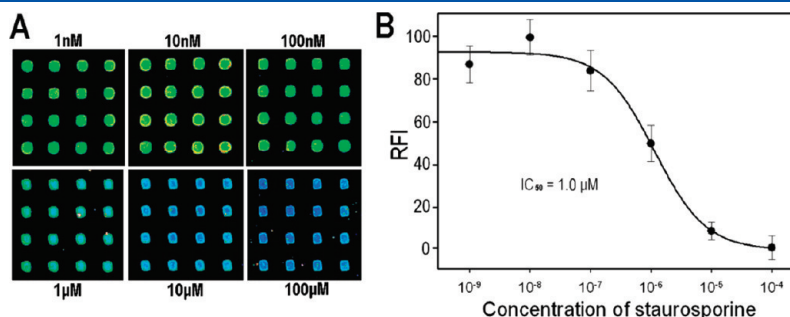


**Figure 6.** Inhibition assay on a p38 $\alpha$ /MBP microarray. Panel A depicts sections of microarrays showing representative spots overspotted with varying concentrations of staurosporine, as indicated. (The images were obtained by a single scan of the same slide; composite image is shown for clarity.) Panel B shows the  $\text{IC}_{50}$  curve generated from the analyzed array images. The intensity obtained at 100  $\mu\text{M}$  was subtracted from all images; all other intensities were normalized by setting the intensity obtained at 10 nM to a value of 100% activity. The intensity gradient is identical to that shown in Figure 3.



criteria to suit specific assays: in the case of kinase microarrays, the detection method placed more-stringent requirements with regard to resistance to cracking upon exposure to assay solutions, levels of nonspecific binding, and the effect of surface chemistry. Interestingly, the 1.4SS/1.0PVA material (optionally with added glycerol) was again identified as a suitable material for printing of active enzyme microarrays, suggesting that this material may be amenable to the printing of a wide variety of proteins.

While we have successfully fabricated pin-printed microarrays, the difficulties associated with producing highly reproducible spots could not be completely resolved. In addition, this printing method results in significant waste of materials, as only a small fraction of the sols are actually printed (e.g., <1% of a typical 40  $\mu$ L reaction volume is needed to print 600 microarray elements when an SMP3 pin is used), and kinases left in the wells could no longer be reused once gelation occurred. This poses a major setback for expensive proteins such as kinases. Thus, contact pin-printing may not be a viable option for high-throughput fabrication of sol–gel-derived microarrays. We are presently investigating other printing methods, specifically non-contact, drop-on-demand printing technology, and the results of these studies will be reported in due course.

## ■ ASSOCIATED CONTENT

**S Supporting Information.** Supporting Information is available as noted in the text. This material is available free of charge via the Internet at <http://pubs.acs.org>.

## ■ AUTHOR INFORMATION

### Corresponding Author

\*Tel.: +1-905-525-9140, ext 27033. Fax: +1-905-527-9950.  
E-mail: [brennanj@mcmaster.ca](mailto:brennanj@mcmaster.ca). Internet: <http://www.chemistry.mcmaster.ca/faculty/brennan/>.

### Present Addresses

<sup>†</sup>Department of Chemical and Environmental Engineering, University of California, Riverside, 900 University Ave., Riverside, CA 92521, USA.

## ■ ACKNOWLEDGMENT

The authors thank the Natural Sciences and Engineering Research Council of Canada (NSERC), the Canada Foundation for Innovation and the Ministry of Research and Innovation, Ontario for funding this work. The authors also thank Millipore Inc. for providing the kinases and substrates used in this study. J.M.L. thanks NSERC for providing a Canada Graduate Scholarship. J.D.B. holds the Canada Research Chair in Bioanalytical Chemistry.

## ■ REFERENCES

- (1) Eglén, R. M.; Reisine, T. *Assay Drug Dev. Technol.* **2009**, *7*, 22–43.
- (2) Hunter, T. *Cell* **1995**, *80*, 225–236.
- (3) Dancey, J.; Sausville, E. A. *Nat. Rev.* **2003**, *2*, 296–313.
- (4) Kumar, S.; Boehm, J.; Lee, J. C. *Nat. Rev.* **2003**, *2*, 717–726.
- (5) Ishii, H.; Koya, D.; King, G. L. *J. Mol. Med.* **1998**, *76*, 21–31.
- (6) Cohen, P. *Curr. Opin. Chem. Biol.* **1999**, *3*, 459–465.
- (7) Klumpp, M.; Boettcher, A.; Becker, D.; Meder, G.; Blank, J.; Leder, L.; Forstner, M.; Ottl, J.; Mayr, L. M. *J. Biomol. Screen.* **2006**, *11*, 617–633.

- (8) Zhu, H.; Klemic, J. F.; Chang, S.; Bertone, P.; Casamayor, A.; Klemic, K. G.; Smith, D.; Gerstein, M.; Reed, M. A.; Snyder, M. *Nat. Genet.* **2000**, *26*, 283–289.
- (9) Reimer, U.; Reineke, U.; Schneider-Mergener, J. *Curr. Opin. Biotechnol.* **2002**, *13*, 315–320.
- (10) Houseman, B. T.; Huh, J. H.; Kron, S. J.; Mrksich, M. *Nat. Biotechnol.* **2002**, *20*, 270–274.
- (11) Rychlewski, L.; Kschischo, M.; Dong, L.; Schutkowski, M.; Reimer, U. *J. Mol. Biol.* **2004**, *336*, 307–311.
- (12) Panse, S.; Dong, L.; Burian, A.; Carus, R.; Schutkowski, M.; Reimer, U.; Schneider-Mergener, J. *Mol. Diversity* **2004**, *8*, 291–299.
- (13) Schutkowski, M.; Reimer, U.; Panse, S.; Dong, L.; Lizcano, J. M.; Alessi, D. R.; Schneider-Mergener, J. *Angew. Chem., Int. Ed.* **2004**, *43*, 2671–2674.
- (14) Min, D. H.; Su, J.; Mrksich, M. *Angew. Chem., Int. Ed.* **2004**, *43*, 5973–5977.
- (15) Rupcich, N.; Green, J. R.; Brennan, J. D. *Anal. Chem.* **2005**, *77*, 8013–8019.
- (16) Cho, E. J.; Bright, F. V. *Anal. Chem.* **2001**, *73*, 3289–3293.
- (17) Cho, E. J.; Tao, Z. Y.; Tehan, E. C.; Bright, F. V. *Anal. Chem.* **2002**, *74*, 6177–6184.
- (18) Lee, M. Y.; Park, C. B.; Dordick, J. S.; Clark, D. S. *Proc. Natl. Acad. Sci., U.S.A.* **2005**, *102*, 983–987.
- (19) Kim, S.; Kim, Y.; Kim, P.; Ha, J. M.; Kim, K.; Sohn, M.; Yoo, J. S.; Lee, J.; Kwon, J. A.; Lee, K. N. *Anal. Chem.* **2006**, *78*, 7392–7396.
- (20) Jin, W.; Brennan, J. D. *Anal. Chim. Acta* **2002**, *461*, 1–36.
- (21) Pierre, A. C. *Biocatal. Biotransform.* **2004**, *22*, 145–170.
- (22) Avnir, D.; Coradin, T.; Lev, O.; Livage, J. *J. Mater. Chem.* **2006**, *16*, 1013–1030.
- (23) Rupcich, N.; Goldstein, A.; Brennan, J. D. *Chem. Mater.* **2003**, *15*, 1803–1811.
- (24) Gill, I.; Ballesteros, A. J. *Am. Chem. Soc.* **1998**, *120*, 8587–8598.
- (25) Rupcich, N.; Brennan, J. D. *Anal. Chim. Acta* **2003**, *500*, 3–12.
- (26) Martin, K.; Steinberg, T. H.; Cooley, L. A.; Gee, K. R.; Beechem, J. M.; Patton, W. F. *Proteomics* **2003**, *3*, 1244–1255.
- (27) Monton, M. R. N.; Lebert, J. M.; Little, J. R. L.; Nair, J. J.; McNulty, J.; Brennan, J. D. *Anal. Chem.* **2010**, *82*, 9365–9373.
- (28) Brook, M. A.; Chen, Y.; Guo, K.; Zhang, Z.; Brennan, J. D. *J. Mater. Chem.* **2004**, *14*, 1469–1479.
- (29) Pro-Q Diamond (P33301), Invitrogen ([www.invitrogen.com](http://www.invitrogen.com)).
- (30) Brinker, C. J.; Scherer, A. R. *Sol–Gel Science: The Physics and Chemistry of Sol–Gel Processing*; Academic Press: San Diego, CA, 1990.
- (31) Hench, L. L.; West, J. K. *Chem. Rev.* **1990**, *90*, 33–72.
- (32) Olson, J. M.; Hallahan, A. R. *Trends Mol. Med.* **2004**, *10*, 125–129.
- (33) Sebolt-Leopold, J. S. *Oncogene* **2000**, *19*, 6594–6599.
- (34) Cohen, P.; Frame, S. *Nat. Rev. Mol. Cell Biol.* **2001**, *2*, 769–776.
- (35) Mendelsohn, J.; Baselga, J. *Oncogene* **2000**, *19*, 6550–6565.
- (36) Kiianitsa, K.; Solinger, J. A.; Heyer, W. D. *Anal. Biochem.* **2003**, *321*, 266–271.
- (37) Cruz-Aguado, J. A.; Chen, Y.; Zhang, Z.; Brook, M. A.; Brennan, J. D. *Anal. Chem.* **2004**, *76*, 4182–4188.
- (38) Wu, P.; Grainger, D. W. *J. Proteome Res.* **2006**, *5*, 2956–2965.